



An Improved Synthesis Process of Ricolinostat: The First Orally Selective HDAC6 Inhibitor

Mengfei Wang^{1,2,3} Niubing Sun^{1,4} Qiushi Chen^{1,2,3} Qingwei Zhang^{1,2,3*}

¹ Shanghai Institute of Pharmaceutical Industry Co., Ltd., China State Institute of Pharmaceutical Industry, Shanghai, People's Republic of China

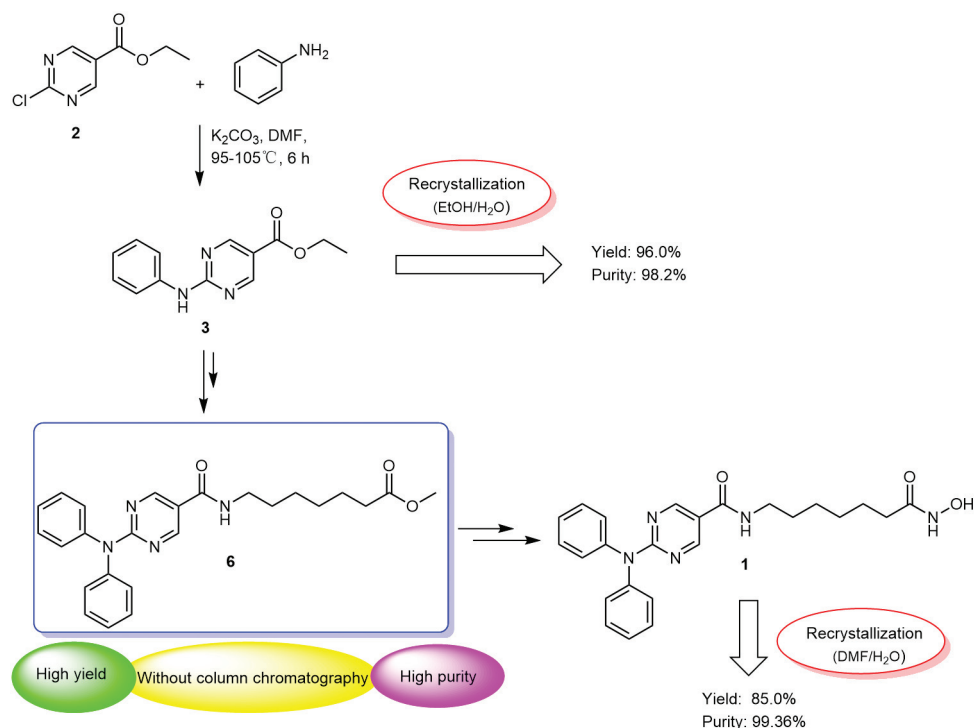
² National Key Laboratory of Lead Druggability Research, Shanghai Institute of Pharmaceutical Industry Co. Ltd., Shanghai, People's Republic of China

³ Shanghai Engineering Research Center of Pharmaceutical Process, Shanghai Institute of Pharmaceutical Industry Co. Ltd., Shanghai, People's Republic of China

⁴ School of Chemistry and Chemical Engineering, Shanghai University of Engineering Science, Shanghai, People's Republic of China

Address for correspondence Qingwei Zhang, PhD, Shanghai Institute of Pharmaceutical Industry Co., Ltd., China State Institute of Pharmaceutical Industry, 285 Gebaini Road, Shanghai 201203, People's Republic of China (e-mail: sipiqingwei@163.com).

Pharmaceut Fronts 2024;6:e430–e438.



received
March 14, 2024
accepted
October 10, 2024
article published online
November 28, 2024

DOI <https://doi.org/10.1055/s-0044-1792125>
ISSN 2628-5088.

© 2024. The Author(s).

This is an open access article published by Thieme under the terms of the Creative Commons Attribution License, permitting unrestricted use, distribution, and reproduction so long as the original work is properly cited. (<https://creativecommons.org/licenses/by/4.0/>)
Georg Thieme Verlag KG, Rüdigerstraße 14, 70469 Stuttgart, Germany

Abstract

Keywords

- ricolinostat
- synthesis process
- recrystallization
- Ullmann reaction

Ricolinostat (**1**) is the first orally available histone deacetylase 6 inhibitor in phase II clinical trials. The results from phase II clinical studies showed that the combination of Ricolinostat with bortezomib and dexamethasone is safe and active for the treatment of multiple myeloma. However, the reported synthesis routes of Ricolinostat were plagued by several limitations, including severe reaction conditions, elevated cost factors, and the employment of environmentally unfriendly reagents. This study aimed to improve the synthesis process of Ricolinostat, in which ethyl 2-chloropyrimidine-5-carboxylate (**2**) was used as the starting material, the target product was obtained through the reaction of nucleophilic aromatic substitution, the Ullmann coupling, hydrolyzation amide condensation, and aminolysis. The nucleophilic substitution (**2** to **3**) was performed in the presence of 1.2 equiv. aniline, 2.0 equiv. K_2CO_3 under $100^\circ C$, with a yield of 96%; the Ullmann reaction was performed in the presence of 0.5 equiv. CuI and 2.0 equiv. cesium carbonate; the post-processes of **3** and the desired product (**1**) that previously required column chromatography were replaced with recrystallization using the solvent of EtOH/ H_2O and DMF/ H_2O , respectively. Through the improved process, Ricolinostat was obtained with an isolated yield of 65.8% and a purity of 99.73%, which was much higher than the reported study. This route was both cost-effective and eco-friendly, making it suitable for industrial applications.

Introduction

Histone deacetylases (HDACs) and histone acetyltransferases regulate gene expression by regulating the levels of histone acetylation in the nucleus.¹ HDACs can be classified into four classes (class I, II, III, and class IV) according to their location and functions.² HDACs play an important role in cancer and have been validated as targets for the development of anticancer drugs.^{3–6} However, in the clinic, most HDAC inhibitors are pan-HDAC inhibitors, with poor activity in solid tumors and significant toxic side effects.⁷

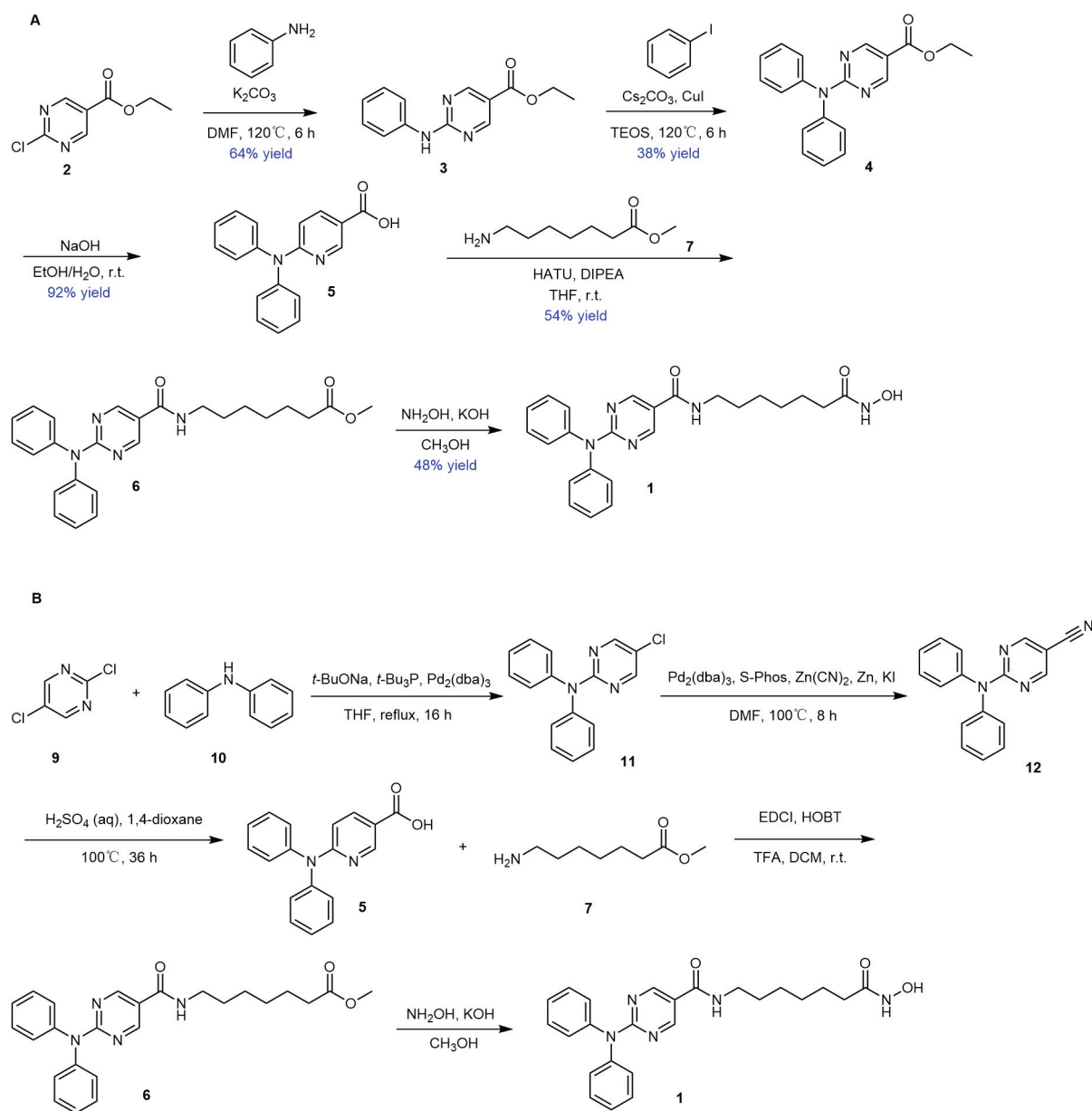
HDAC6 is the most unique member of the class II family of HDACs, mainly expressed in the cytoplasm and perinucleus, and highly expressed in the brain, heart, liver, kidney, and other organs.^{8–10} HDAC6 is involved in a variety of intracellular physiological processes. It not only has strong HDAC activity but also mediates non-histone deacetylation.¹¹ Its main substrates include α -tubulin, Bax, heat shock protein 90, HIF1 α , GRK2, p300, cortical actin, etc.^{12,13} It also interacts with VCP, nuclear factor- κB , Foxp3, tau, protein phosphatase 1, Ku70, PCK α , etc., and is involved in regulating cell morphology, autophagy, migration, and oxidative stress protection. Evidence suggests that overexpression of HDAC6 is closely related to a variety of disorders, including cancer, autoimmune diseases, neurodegenerative diseases, viral infections, and dilated cardiomyopathy.^{14,15} However, mice that knocked out HDAC6 survived well and developed normally, suggesting that selective inhibition of HDAC6 may not cause serious toxic effects.¹⁶

Ricolinostat is the first and most advanced selective HDAC6 inhibitor and is currently in a phase II clinical trial. The results from the Phase Ib clinical studies showed that Ricolinostat is a safe and well-tolerated HDAC6 inhibitor

with antitumor activities in a wide range of cancers including glioblastoma, multiple myeloma, and melanoma.¹⁷ The combination of Ricolinostat with bortezomib and dexamethasone is safe and active at the recommended phase II dose of 160 mg per day, suggesting that Ricolinostat is a promising approach for the treatment of multiple myeloma.¹⁸

Ricolinostat can be synthesized according to reported studies since 2018. Moore and Min¹⁹ synthesized Ricolinostat (**1**) using ethyl 2-chloropyrimidine-5-carboxylate **2** as a starting material. Cuprous iodide (CuI)-catalyzed Ullmann reaction of the derivated ethyl 2-(phenylamino)pyrimidine-5-carboxylate (**3**) with iodobenzene afforded 2-(diphenylamino)pyrimidine intermediate (**4**). Hydrolysis of **4** in the presence of sodium hydroxide afforded the acid intermediate **5**, which was condensed with methyl 7-aminoheptanoate (**7**) to afford the amide (**6**). Aminolysis of **6** with hydroxylamine provided the target compound Ricolinostat (**1**) (► **Scheme 1A**).¹⁹ However, column chromatography was repeatedly used in the separations, thereby limiting the widespread application of this route. Li et al synthesized Ricolinostat using 2,5-dichloropyrimidine (**9**) and diphenylamine (**10**) as starting materials (► **Scheme 1B**).²⁰ The key steps include two steps of the Buchwald–Hartwig cross-coupling reaction to give the target product. However, the overall yield was only 47.3%. In addition, the use of poisonous reagents (e.g., $Zn(CN)_2$) in the cyanation reaction is environmentally unfriendly, and expensive transition metal catalysts (e.g., $Pd_2(dba)_3$) again limit the large-scale industrial synthesis of Ricolinostat (**1**).

This study aimed to explore a synthesis method suitable for the industrial production of Ricolinostat (**1**). In this work, the synthesis route of Ricolinostat (**1**) in ► **Scheme 1A** was optimized. We focused on solving problems as follows: (1) improving the reaction conditions of nucleophilic



Scheme 1 Reported synthesis routes of Ricolinostat.

substitution (2 to 3); (2) improving the reaction conditions of the Ullmann reaction (3 to 4); (3) using recrystallization instead of all column chromatography for purification.

Results and Discussion

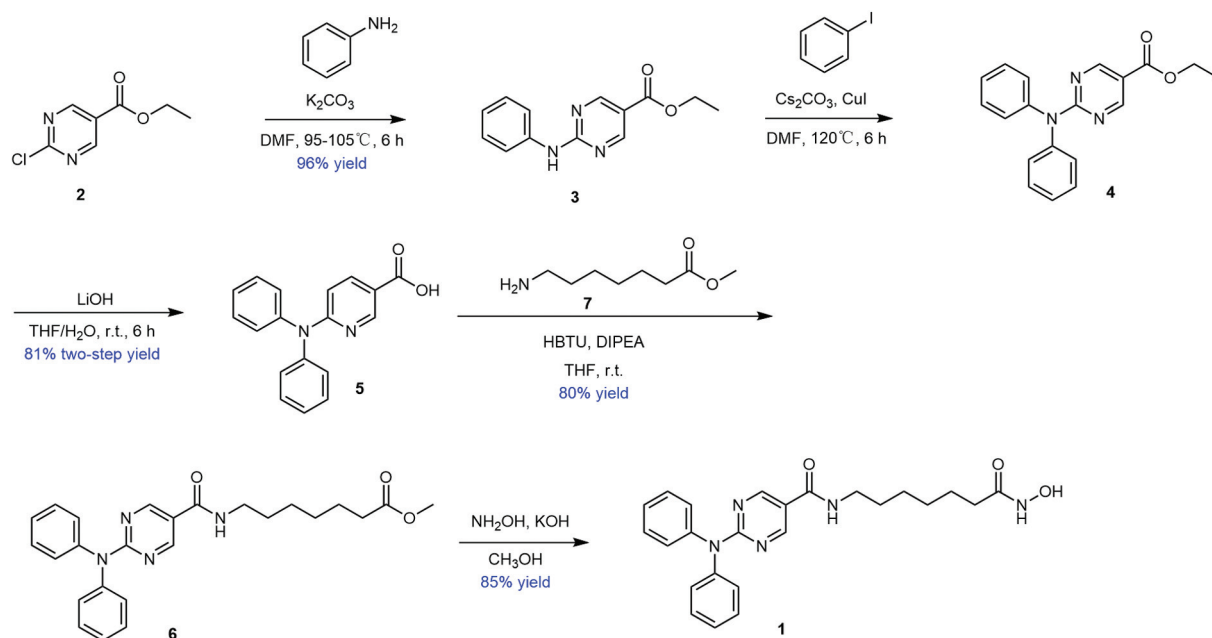
Synthesis Route of Ricolinostat (1)

As shown in **Scheme 2**, the commercially available **2** was reacted with aniline to afford intermediate **3**, which then reacted with iodobenzene through the Ullmann reaction to afford intermediate **4** without any purification. Hydrolysis of **4** in the solution of lithium hydroxide afforded the acid intermediate **5**, which was then condensed with methyl-7-aminoheptanoate **7** to achieve the amide **6**. Aminolysis of **6** with hydroxylamine provided the target compound Ricolinostat **1**. We optimized the nucleophilic substitution (2 to

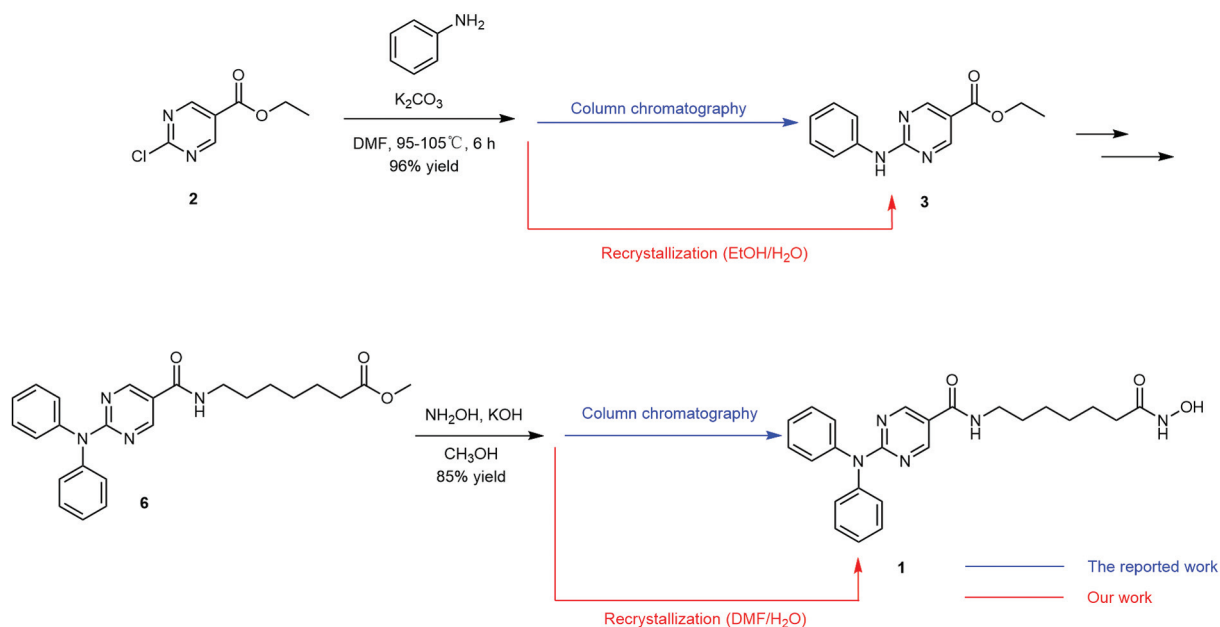
3), the Ullmann reaction (**3** to **4**) as well as the post-processes (**3** and **1**) that require column chromatography and used recrystallization instead (**Scheme 3**). Overall, this optimized synthesis route was operated easily and was able to deliver the product with a yield of 65.8% and a purity of 99.73%, which was much higher than the reported study (6%).¹⁹

Optimization of the Nucleophilic Substitution (2 to 3)

Ethyl 2-(phenylamino)pyrimidine-5-carboxylate (**3**) can be obtained from the reaction of **2** with aniline.^{21,22} In this work, the equiv. of aniline was screened. We started an investigation with 1.0 equiv. of aniline, following the reported research (**Table 1**, entry 1).^{23,24} When the equiv. of aniline was increased, the isolated yield of compound **3** was enhanced, with the maximum effect being seen in 1.2



Scheme 2 Improved synthesis route of Ricolinostat in this work.



Scheme 3 Optimization of post-processes that require column chromatography.

equiv. When the equiv. exceeds 1.2 equiv., the yield did not increase significantly (data are not available here). Thus, 1.20 equiv. of aniline was chosen in the reaction.

Temperature is closely related to energy consumption and production costs in the pharmaceutical industry. We attempt to explore an appropriate reaction temperature suitable for scale-up. The initial refluxed condition was 135 to 125°C (► Table 2, entry 1) according to a reported study.¹⁹ Reducing the temperature to 125 to 105°C had essentially no impact (► Table 2, entries 2 – 3). Reducing the temperature to 105 to 95°C resulted in a longer reaction time (► Table 2, entry 4).

Reducing the temperature to 95 to 85°C resulted in incomplete conversion (► Table 2, entry 5). Therefore, the optimal temperature was found to be 105 to 95°C.

Optimization of the Ullmann Reaction Catalyzed by Copper(I) Iodide (3 to 4)

N-Aryl amine moieties are important structural features that are ubiquitously found in numerous natural products, pharmaceuticals, agrochemicals, and material molecules.²⁵ A typical approach for preparing *N*-aryl amines is the copper-catalyzed Ullmann coupling reaction of aryl halides with

Table 1 Screening aniline (equiv.) for the nucleophilic substitution^a

Entry	Aniline (equiv.)	Yield (%) ^b
1	1.00	72.4
2	1.05	82.5
3	1.10	90.3
4	1.15	95.5
5	1.20	98.8

^aReaction conditions: **2** (10 g scale, 1.0 equiv.), K₂CO₃ (1.5 equiv.), DMF (5 V).

^bIsolated yields.

Table 2 Screening temperature for the nucleophilic substitution^a

Entry	Temperature (°C)	Time (h)	Conversion (%) ^b
1	135–125	4	100
2	125–115	4	100
3	115–105	8	100
4	105–95	8	100
5	95–85	16	53.9

^aReaction conditions: **2** (10 g scale, 1.0 equiv.), aniline (1.2 equiv.), DMF (5 V).

^bMeasured by HPLC.

amines.²⁶ Traditionally, the reaction requires a high reaction temperature and a stoichiometric amount of copper reagent, greatly limiting the reaction scope.²⁷ In this work, the Ullmann reaction of **3** to produce **4** was optimized.

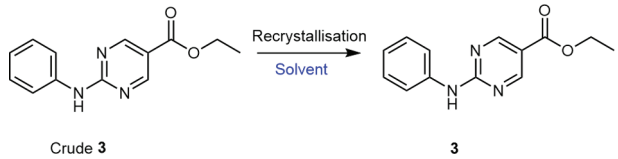
Catalysis types were screened due to the low yield in the reported study. In our preliminary study, Pd₂(dba)₃, PdCl₂(PPh₃)₂, Pd(PPh₃)₄, Cu₂O, and CuI were screened for the Ullmann reaction, and we found that the copper(I) iodide from the reported study showed the best catalytic efficiency, but a small amount of starting material **3** remained (►Table S1, Supporting Information [available in the online version]). Fortunately, we found that increasing the amount of copper(I) iodide could improve the conversion. When the amount of copper(I) iodide increased to 0.5 equiv., the substrate could be completely converted in the reaction.

The catalysis activity can be influenced by the types of the bases.^{28,29} In the present study, an investigation of alkalis was performed in the range of organic bases and inorganic

bases (►Table S2, Supporting Information [available in the online version]) and the results showed that cesium carbonate was the most effective. The reported literature used tetraethoxysilane (TEOS) as a solvent, which was unstable in the presence of water and had irritant properties. Therefore, we considered changing the solvent and chose *N,N*-dimethylformamide (DMF) as an alternative. Given the above, we selected copper(I) iodide (1.5 equiv.) as the catalysis, cesium carbonate as the base, and DMF as the solvent for the reaction in a 105 g scale, producing the target product with an isolated yield of 80.5% and a purity of 98.86%.

Optimization of Post-processes That Require Column Chromatography

In the context of industrial production, the simplicity of post-processing becomes the most critical variable and requires careful consideration. However, the reported routes required at least one step of column chromatography, which is not

Table 3 Screening recrystallization solvent for **3**^a


Entry	Recrystallization solvent and volume	Yield (%) ^b	Purity (%) ^c
1	EtOH/H ₂ O (5V/4V)	31.1	96.56
2	EtOH (20V)	21.8	99.22
3	H ₂ O (15V)	48.8	99.45
4	EtOH/H ₂ O (10V/7V)	32.1	98.09
5	EtOH/H ₂ O (10V/6V)	41.0	98.44
6	EtOH/H ₂ O (10V/5V)	47.2	98.95
7	EtOH/H ₂ O (10V/4V)	95.8	99.36
8	EtOH/H ₂ O (10V/3V)	60.0	99.08

^a3.0 g scale of crude **3** was used for recrystallization.

^bIsolated yields.

^cMeasured by HPLC.

suitable for industrial production. Therefore, we optimized post-processes. In this work, we succeeded in eliminating two steps of column chromatography and used recrystallization instead (**Scheme 3**).

Different recrystallization systems of crude **3** were investigated (**Table 3**). Under the EtOH/H₂O (5 V/4V) recrystallization system, the purity of **3** was 96.56%, but the isolated yield was only 31.1%. However, when EtOH or H₂O was used as a single recrystallization solvent, the isolated yields of **3** were not satisfactory (21.8 and 48.8%, respectively) (**Table 3**, entries 2–3). Then, different ratios of EtOH/H₂O were screened. Our data showed that when EtOH/H₂O (10 V/7V) was used as the solvent, the isolated yield and purity of **3** were 32.1 and 98.09%, respectively (**Table 3**, entry 4). The reduction of water ratio in the mixing solvent affected the yield and purity of the product, with the EtOH/H₂O (10 V/4V) recrystallization system giving the best result (**Table 3**, entry 5). Under this recrystallization system, **3** was obtained with an isolated yield of 95.8% and a purity of 99.36% on a 150 g scale.

This work reported the purification of Ricolinostat (**1**) by recrystallization for the first time. The data showed that under the DMF/dichloromethane (DCM) recrystallization system, the isolated yield of **1** was poor, with the best result of only 35% (**Table 4**, entries 1–5). However, under the H₂O/DMF (10:1, v:v) recrystallization system, **1** was obtained with an isolated yield of 85.0% and a purity of 99.73% on a 50.0 g scale (**Table 4**, entries 6–7).

Conclusion

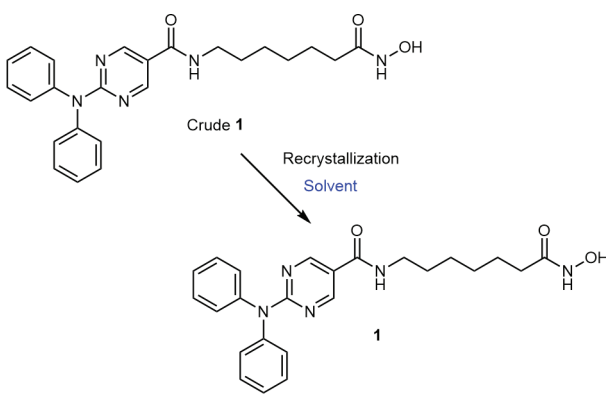
In this work, we optimized the synthesis route of Ricolinostat (**1**). First, by investigating the equiv. of aniline and the temper-

ature of the nucleophilic substitution reaction, a process for efficient construction of compound **3** was established. Second, by screening the types of catalysts and alkalis of the Ullmann coupling, the synthesis process of compound **4** was optimized. Finally, the recrystallization methods for the purification of compound **3** and Ricolinostat (**1**) were successfully established, which gave **3** a purity of 99.36% and Ricolinostat a purity of 99.73%. The improved synthesis route is able to deliver a product with an isolated yield of 65.8% over five steps and has been found to be both cost-effective and eco-friendly, making it suitable for industrial applications.

Experimental Section

General Method

All reagents were commercially available, and were purchased from Shanghai BiDe PharmaTech Co., Sinopharm Co., Shanghai Haohong Bio-medical Technology Co., etc., and used without further purification unless indicated otherwise. High-performance liquid chromatography (HPLC) analysis was conducted on a Dionex UltiMate 3000 HPLC (Dionex, United States) using an Agilent Eclipse plus C18 column (4.6 mm × 250 mm, 5 μm, Agilent, United States). Mobile A was aqueous sodium octane sulfonate (15 mmol/mL, pH 3.30 ± 0.2)-acetonitrile (90:10, v/v); and mobile B was acetonitrile. The gradient program was as follows: 0–25 minutes, 15% B; 25–30 minutes, 60% B; 30–31 minutes, 15% B; 31–40 minutes, 15% B. The flow rate was 1.0 mL/min, the column temperature was 30°C, and UV detection at 215 nm. Nuclear magnetic resonance (NMR) spectra were recorded on a Bruker 400 spectrometer (Bruker, Germany). Chemical shifts (δ) were given in parts

Table 4 Screening recrystallization solvent for 1^a


Entry	Solvent	Volumes	Yield (%) ^b	Purity (%) ^c
1	DCM/DMF (9:1)	5 V	–	–
2	DCM/DMF (9:1)	10 V	–	–
3	DCM/DMF (4:1)	5 V	–	–
4	DCM/DMF (4:1)	10 V	–	–
5	DCM/DMF (1:1)	5 V	35.5	98.7
6	H ₂ O/DMF (10:1)	5 V	–	–
7	H ₂ O/DMF (10:1)	10 V	85.0	99.73

^a3.0 g scale of crude 3 was used for recrystallization.

^bIsolated yields.

^cMeasured by HPLC.

per million (ppm) and referenced to the residual protonated solvent peak (DMSO-*d*₆: 2.50 ppm for ¹H NMR and 39.53 ppm for ¹³C NMR or chloroform-*d*: 7.26 ppm for ¹H NMR and 77.1 ppm for ¹³C NMR). Multiplicities are abbreviated as singlet (s), doublet (d), triplet (t), quartet (q), and multiplet (m). Coupling constants (*J*) are reported in Hertz (Hz).

Ethyl 2-(Phenylamino) Pyrimidine-5-carboxylate (3)

Ethyl 2-chloropyrimidine-5-carboxylate **2** (138.0 g, 740 mmol) was added to a 5.0 L four-necked flask. Then DMF (1000 mL) was added and mechanically stirred. K₂CO₃ (204.4 g, 1480 mmol) and aniline (82.6 g, 888 mmol) were sequentially charged into a four-necked flask under N₂. The reaction mixture was stirred at 100°C for 8 hours. After completion conversion of compound **2** as determined by HPLC, the reaction mixture was gradually cooled to 25°C, ice water (2.0 L) was added, and stirred for 30 minutes. The precipitated solid was collected by filtration. The cake was washed with water and dried at 60°C to afford compound **3** (95.9% isolated yield, 99.36% HPLC purity) as a white solid. ¹H NMR (600 MHz, DMSO-*d*₆) δ 10.34 (s, 1H), 8.90 (s, 2H), 7.83–7.68 (m, 2H), 7.41–7.27 (m, 2H), 7.05 (tt, *J* = 7.3, 1.2 Hz, 1H), 4.30 (q, *J* = 7.1 Hz, 2H), 1.31 (t, *J* = 7.1 Hz, 3H). ¹³C NMR (DMSO-*d*₆) δ 165.42, 161.74, 159.91, 140.22, 130.36, 123.36, 118.98, 114.39, 60.96, 15.71.

Ethyl 2-(diphenylamino) Pyrimidine-5-carboxylate (4)

Ethyl 2-(phenylamino) pyrimidine-5-carboxylate (**3**) (1,500 g, 617 mmol) was added to a 5.0 L four-necked flask, then, DMF (2.0 L) was added and mechanically stirred. Iodobenzene (188.0 g, 926 mmol), cuprous iodide (58.8 g, 308 mmol), and cesium carbonate (402.1 g, 1234 mmol) were charged sequentially under N₂. The reaction mixture was stirred at 130°C for 5 hours. After complete conversion of compound **3** as determined by HPLC, the reaction solution was gradually cooled to 25°C, and ethyl acetate (EA; 3.5 L) was added. Thereafter, the mixture was filtered. The mother liquid was extracted with EA after the addition of water (2.0 L). The organic layers were combined, washed with water, and concentrated to produce crude **4**, which was used for the next step without further purification. ¹H NMR (400 MHz, chloroform-*d*) δ 8.90 (s, 2H), 7.39 (dd, *J* = 8.4, 7.2 Hz, 4H), 7.34–7.20 (m, 6H), 4.34 (q, *J* = 7.1 Hz, 2H), 1.35 (t, *J* = 7.1 Hz, 3H).

2-(Diphenylamino) Pyrimidine-5-carboxylic Acid (5)

Ethyl 2-(diphenylamino) pyrimidine-5-carboxylate (**4**) (a crude product, theoretical yield: 196.9 g, 617 mmol) was added to a 5.0 L four-necked flask. A mixture of water and THF (1:1, 2.6 L) was added and mechanically stirred at 350 rpm. LiOH (77.7 g, 1,851 mmol) was added. The reaction mixture was stirred at ambient temperature for 8 hours

until complete conversion of compound **4** as determined by HPLC. The THF was removed under vacuum. The aqueous layer was extracted with DCM and adjusted pH to 5.5. The precipitated solid was filtered and washed with water to obtain compound **5** (80.5% isolated yield, 98.86% HPLC purity) as a white solid. ¹H NMR (600 MHz) δ 13.06 (s, 1H), 8.77 (s, 2H), 7.42–7.38 (m, 4H), 7.38–7.32 (m, 4H), 7.27 (td, *J* = 7.3, 1.3 Hz, 2H).

Methyl 7-[[[2-(diphenylamino)-5-pyrimidinyl]carbonyl]amino]heptanoate (**6**)

DIPEA (504.0 g, 3897 mmol) and HBTU (364.0 g, 1134 mmol) were sequentially added to a solution of compound **5** (300.0 g, 1,031 mmol) and methyl 7-aminoheptanoate (**7**) (293.0 g, 1,495 mmol) in THF (1.5 L). The reaction mixture was stirred at room temperature for 8 hours, removed THF under vacuum, and then extracted with EA/water. The organic layers were combined, washed with water, and concentrated to produce crude **6** as a yellow oily liquid, which was used for the next step without further purification. ¹H NMR (600 MHz, DMSO-*d*₆) δ 8.73 (s, 2H), 8.39 (t, *J* = 5.6 Hz, 1H), 7.44–7.36 (m, 4H), 7.35–7.28 (m, 4H), 7.28–7.22 (m, 2H), 3.58 (s, 3H), 3.23 (q, *J* = 6.6 Hz, 2H), 2.29 (t, *J* = 7.4 Hz, 2H), 1.51 (dq, *J* = 18.7, 7.1 Hz, 4H), 1.30 (dt, *J* = 7.9, 3.3 Hz, 4H).

Ricolinostat (**1**)

Hydroxylamine hydrochloride (25.0 g, 360 mmol) and CH₃OH were added in one portion to a 500 mL flask. A CH₃OH solution containing KOH (125.0 mL; 22.3 g, 400 mmol) was added dropwise at 0°C, stirred at 0°C for 30 minutes, and filtered. Mother liquor was collected. Compound **5** (44.54 g, 103 mmol) was added to the mother liquor. CH₃OH solution containing KOH was added dropwise at 0°C. Stirring was continued until HPLC determined the complete conversion of compound **5**. Removing CH₃OH under vacuum afforded a yellow oily liquid, which was recrystallized by DMF/H₂O (DMF: H₂O = 1:1, 10 V) at 70°C. The precipitated solid was filtered to obtain compound **1** (85.2% isolated yield, 99.36% purity) as a white solid. ¹H NMR (400 MHz, DMSO-*d*₆) δ 10.33 (d, *J* = 1.7 Hz, 1H), 8.72 (s, 2H), 8.66 (d, *J* = 1.5 Hz, 1H), 8.40 (t, *J* = 5.6 Hz, 1H), 7.47–7.35 (m, 4H), 7.35–7.18 (m, 6H), 3.22 (q, *J* = 6.6 Hz, 2H), 1.93 (t, *J* = 7.4 Hz, 2H), 1.48 (p, *J* = 7.0 Hz, 4H), 1.26 (p, *J* = 6.3, 5.2 Hz, 4H). ¹³C NMR (DMSO-*d*₆) δ 169.05, 162.91, 157.70, 144.63, 129.68, 127.77, 126.52, 120.99, 32.67, 29.47, 28.77, 28.62, 25.52. ESI-MS (*m/z*): calcd. for C₂₄H₂₈N₅O₃⁺ [M + H]⁺ 434.2114; found 434.2.

Supporting Information

Screening results of catalysts and alkalis for the Ullmann reaction (► Tables S1 and S2 [available in the online version]) as well as ¹H NMR, ¹³C NMR, MS, and HPLC spectra of compounds **3** and **1** (► Fig. S1–S8 [available in the online version]) can be found in the “Supporting Information” section of this article’s webpage.

Funding

This work was supported by the National Science and Technology Major Project (Grant No. 2018ZX09711002-002-009), the National Natural Science Foundation of China (Grant No. 81703358), the Science and Technology Commission of Shanghai Municipality (Grant Nos. 17431903900, 18QB1404200, 21S11908000, 22ZR146-0300, 23DZ2292600), and the National Key Laboratory of Lead Druggability Research (Grant No. NKLYT2023001).

Conflict of Interest

None declared.

References

- Wang J, Feng S, Zhang Q, et al. Roles of histone acetyltransferases and deacetylases in the retinal development and diseases. *Mol Neurobiol* 2023;60(04):2330–2354
- Blixt NC, Faulkner BK, Astleford K, et al. Class II and IV HDACs function as inhibitors of osteoclast differentiation. *PLoS One* 2017;12(09):e0185441
- Gu X, Peng X, Zhang H, et al. Discovery of indole-containing benzamide derivatives as HDAC1 inhibitors with *in vitro* and *in vivo* antitumor activities. *Pharmaceutical Fronts* 2022;4:e61–e70
- Jiao M, Han B, Gu X, et al. Design, synthesis, and evaluation of benzoheterocyclic-containing derivatives as novel HDAC1 inhibitors. *Pharmaceutical Fronts* 2022;4:e22–e29
- König B, Watson PR, Reßing N, et al. Difluoromethyl-1,3,4-oxadiazoles are selective, mechanism-based, and essentially irreversible inhibitors of histone deacetylase 6. *J Med Chem* 2023;66(19):13821–13837
- Zhang Z, Zhang Q, Zhang H, et al. Discovery of quinazolinyl-containing benzamides derivatives as novel HDAC1 inhibitors with *in vitro* and *in vivo* antitumor activities. *Bioorg Chem* 2021;117:105407
- Xiong K, Zhang H, Du Y, Tian J, Ding S. Identification of HDAC9 as a viable therapeutic target for the treatment of gastric cancer. *Exp Mol Med* 2019;51(08):1–15
- Gu X, Zhang H, Jiao M, et al. Histone deacetylase 6 inhibitors with blood-brain barrier penetration as a potential strategy for CNS-Disorders therapy. *Eur J Med Chem* 2022;229:114090
- Han B, Wang M, Li J, et al. Perspectives and new aspects of histone deacetylase inhibitors in the therapy of CNS diseases. *Eur J Med Chem* 2023;258:115613
- Liang T, Fang H. Structure, functions and selective inhibitors of HDAC6. *Curr Top Med Chem* 2018;18(28):2429–2447
- Lee YS, Lim KH, Guo X, et al. The cytoplasmic deacetylase HDAC6 is required for efficient oncogenic tumorigenesis. *Cancer Res* 2008;68(18):7561–7569
- Zhang X, Yuan Z, Zhang Y, et al. HDAC6 modulates cell motility by altering the acetylation level of cortactin. *Mol Cell* 2007;27(02):197–213
- Kovacs JJ, Murphy PJ, Gaillard S, et al. HDAC6 regulates Hsp90 acetylation and chaperone-dependent activation of glucocorticoid receptor. *Mol Cell* 2005;18(05):601–607
- Li T, Zhang C, Hassan S, et al. Histone deacetylase 6 in cancer. *J Hematol Oncol* 2018;11(01):111
- LoPresti P. The selective HDAC6 inhibitor ACY-738 impacts memory and disease regulation in an animal model of multiple sclerosis. *Front Neurol* 2019;10:519
- Zanin M, DeBeauchamp J, Vangala G, Webby RJ, Husain M. Histone deacetylase 6 knockout mice exhibit higher susceptibility to influenza a virus infection. *Viruses* 2020;12(07):728
- Amengual JE, Prabhu SA, Lombardo M, et al. Mechanisms of acquired drug resistance to the HDAC6 selective inhibitor

- ricolinostat reveals rational drug-drug combination with ibrutinib. *Clin Cancer Res* 2017;23(12):3084–3096
- 18 Vogl DT, Raje N, Jagannath S, et al. Ricolinostat, the first selective histone deacetylase 6 inhibitor, in combination with bortezomib and dexamethasone for relapsed or refractory multiple myeloma. *Clin Cancer Res* 2017;23(13):3307–3315
 - 19 Moore N, Min C. Pharmaceutical combinations comprising a histone deacetylase inhibitor and a BCL-2 inhibitor and methods of use thereof. WO Patent 2018085652. May, 2018
 - 20 Li J, Zhang Q, Guo Z, Pu Q, Zeng J, Qian H. Sulfhydryl compound as histone deacetylase inhibitor and composition and application in preparing medicine for treating diseases caused by abnormal gene expression thereof [in Chinese]. CN Patent 110885316 A. March, 2020
 - 21 Deng Z, Fan W, Liu J, et al. A novel approach to α -arylacetonitrile skeletons via para-selective alkylation of protected anilines. *Chemistry* 2023;29(44):e202300905
 - 22 Quayle S, Jones SS, Hideshima T, Anderson KC. Pharmaceutical combinations comprising a histone deacetylase inhibitor and a programmed death-ligand 1 (PD-L1) inhibitor and methods of use thereof. WO Patent 2018098168. May, 2018
 - 23 Pozzi S, Cosenza M, Civallero M. Methods of use and pharmaceutical combinations comprising histone deacetylase inhibitors and JAK1/2 inhibitors. WO Patent 2019106633. June, 2019
 - 24 Raje N, Santo L. Preparation of hydroxamic acid derivatives as histone deacetylase 6 selective inhibitors for the treatment of bone disease. WO Patent 2013013113. March, 2013
 - 25 Lygaitis R, Getautis V, Grazulevicius JV. Hole-transporting hydrazones. *Chem Soc Rev* 2008;37(04):770–788
 - 26 Hassan J, Sévignon M, Gozzi C, Schulz E, Lemaire M. Aryl-aryl bond formation one century after the discovery of the Ullmann reaction. *Chem Rev* 2002;102(05):1359–1470
 - 27 Bariwal J, Van der Eycken E. C-N bond forming cross-coupling reactions: an overview. *Chem Soc Rev* 2013;42(24):9283–9303
 - 28 Ali MH, Buchwald SL. An improved method for the palladium-catalyzed amination of aryl iodides. *J Org Chem* 2001;66(08):2560–2565
 - 29 Li JJ, Wang Z, Mitchell LH. A practical Buchwald-Hartwig amination of 2-bromopyridines with volatile amines. *J Org Chem* 2007;72(09):3606–3607